PROGRESS IN PHOTOVOLTAICS: RESEARCH AND APPLICATIONS
Prog. Photovolt: Res. Appl. 2000; **8**:363–375

Research

Reduced Fill Factors in Multicrystalline Silicon Solar Cells Due to Injection-level Dependent Bulk Recombination Lifetimes

Daniel Macdonald* and Andres Cuevas
Department of Engineering, FEIT, Australian National University, ACT 0200, Australia

Recombination lifetimes of multicrystalline silicon solar cell precursors have been measured experimentally as a function of injection-level, and modeled using Shockley–Read–Hall statistics. The expressions for the variable lifetimes are then used to predict the final cell open-circuit voltages and fill factors using a simple analytic method. When accurate recombination lifetimes measurements are possible, the predicted parameters match well with the measured values on finished cells. The cells are shown to be limited by the presence of bulk recombination, which not only limits the open-circuit voltage through lower lifetimes, but also reduces the fill factor due to a strong injection-level dependence around one-sun maximum-power conditions. It is shown that such non-ideal behaviour cannot be adequately explained by junction recombination. The specific effect of interstitial iron, an important impurity in silicon, on voltages and fill factors is modeled numerically and discussed.

INTRODUCTION

MULTICRYSTALLINE silicon (mc-Si) solar cells have achieved excellent results recently using high-efficiency cell designs.[1,2] However, they still fall well short of the records achieved on single-crystal silicon. It is useful then, to compare the limiting mechanisms in these two types of cell in order to illuminate the path to further improvements. For the ultra-high efficiency single-crystal cells, it has been shown that the primary factor limiting the open-circuit voltages is bulk recombination in the base.[3] Performance is further decreased by the injection-level dependence of the surface recombination velocity of the rear oxide, which leads to a 'kink' in the J_{SC}–V_{OC} curve, resulting in ideality factors greater than unity, and hence lower fill factors.[4,5]

In this paper we examine the limiting mechanisms in similar high-efficiency mc-Si cells. The recombination lifetimes of cell precursors have been determined experimentally as a function of injection-level, and modeled with Shockley–Read–Hall (SRH) statistics and an emitter recombination term. Analysis of the results shows that the voltages are primarily limited by recombination in the bulk of

* Correspondence to: Daniel Macdonald, Department of Engineering, FEIT, Australian National University, ACT 0200, Australia. E-mail: daniel@faceng.anu.edu.au

Received 10 January 2000
Revised 3 March 2000

the cells, as with the single-crystal cells mentioned above. However, the behaviour of these bulk SRH centres has a similar effect to the surface recombination velocity of the rear oxide in the single-crystal cells. Specifically, the bulk lifetimes exhibit a strong injection-level dependence which leads to a hump in the illumination-V_{OC} curve. Importantly, the injection-level dependence around one-sun maximum-power conditions is very strong, resulting in ideality factors greater than unity and therefore causing reduced one-sun fill factors. Note that the quality of the rear surface passivation of these cells is similar to that of the single-crystal cells, but since the bulk lifetimes are significantly lower, the rear surface has a negligible impact on cell parameters.

Using a simple analytic method to convert the lifetime measurements into implied I–V curves, we find that the measured fill factors and voltages agree well with the predicted values, provided the devices satisfy certain conditions. Conventionally, ideality factors greater than unity have been explained by the presence of junction recombination. However, we find, similar to Aberle *et al.*,[4] that such an explanation is not valid for these cells. The non-idealities and hence reduced fill factors are explained much more plausibly, in this case, by the bulk lifetime injection-level dependence.

The practical implications of these findings are important. Commercial solar grade mc-Si often contains lifetime limiting quantities of metallic impurities, particularly iron.[6] Although gettering by emitter and Al back-surface-field formation helps to reduce the impurity content in the bulk,[7] there often still remain enough impurities to limit the bulk lifetime. We use the electron- and hole-capture cross-sections for interstitial Fe (Fe_i), as reported in the literature, to accurately model its effect on open-circuit voltages and fill factors, using the finite element analysis program PC1D. The detrimental impact of these centres on fill factors is shown to be significant, even for low Fe_i concentrations, due primarily to the large asymmetry between the capture cross-sections.

EXPERIMENTAL METHODS

Solar cells were fabricated on 1·5 and 0·4 Ω cm boron-doped cast mc-Si wafers grown by directional solidification at Eurosolare, Italy. High-efficiency cell structures were used to ensure good sensitivity to bulk lifetime dependence in the cells. Photolithographically-defined contacts on lightly-doped (>100 Ω/square), oxide-passivated emitters ensured low emitter recombination losses. Point-contacts through an aluminium-annealed (alnealed) oxide on the rear of the cells similarly afforded very low rear-surface recombination losses.[8] Edge effects were avoided through the use of planar diffusions through a 4 cm^2 window in a thermal oxide extending well beyond the cell boundaries.

Lifetime measurements were performed using the quasi-steady-state photoconductance (QSSPC) technique.[9] Such a technique is well suited to predicting wafer-averaged cell parameters from lifetimes on highly inhomogeneous materials like mc-Si, since the steady-state nature of the method ensures that both high and low lifetime regions contribute with appropriate weight to the total result. Hence the effect of grain boundaries for example are implicitly taken account of. This is often not the case for transient methods, which tend to over-estimate lifetimes on inhomogeneous materials due to the rapid decay of the signal in poor regions. Recently, an improved, more general method for analyzing QSSPC data has been developed,[10] which enables reliable measurement of lifetimes ranging from 1 μs to above 1 ms, over an injection-level range from around 1×10^{12} to about 5×10^{16} cm^{-3}, depending on the magnitude of the lifetime.

It is well known that recombination lifetimes can be affected significantly by cell fabrication processes. This is particularly true for mc-Si, which is often prone to lifetime degradation during high temperature steps such as oxidations.[11] As a result, in order to make accurate corelations between substrate lifetimes and final cell parameters, it is crucial that the lifetime measurements be performed near the end of the fabrication process. Since the presence of metal contacts makes accurate excess-photoconductance measurements impossible on our system, lifetimes were measured just prior to metallization and immediately after the opening of contact-holes through the front and rear (alnealed) passivating oxides. To verify that the metallization process did not impact on the substrate lifetime, the contacts were

removed on one of the finished cells and the lifetimes re-measured. The results revealed no discernible change.

After metallization, the one-sun I–V curves of the cells were measured, as were their illumination-V_{OC} profiles. The latter was achieved by monitoring the open-circuit voltage on an oscilloscope while simultaneously monitoring the intensity of an exponentially decaying flash-lamp.[12]

ANALYTIC MODELING TECHNIQUES

Recombination lifetimes in solar cell precursors are affected by a number of different mechanisms which tend to dominate under different injection-level conditions. Under low- to mid-injection, the recombination lifetime is dominated by multiphonon-assisted recombination through defect states, a phenomenon which is frequently characterized by Shockley–Read–Hall (SRH) statistics.[13–15] This approach can be used to model defect-related recombination at a surface (in the form of a surface recombination velocity), or in the bulk. Often the combined effects of more than one SRH centre need to be included to accurately describe experimental data.[16] From mid- to high-injection, recombination in the emitter tends to dominate. At very high injection-levels, or in very heavily-doped samples, Auger recombination becomes the most important recombination mechanism. However, due to the low defect-related lifetimes in our samples (<100 μs), and the fact that the cells operate in low injection, Auger recombination plays no role in these devices, and is subsequently neglected. Also, the passivating quality of the alnealed oxides was sufficiently high to ensure that recombination at the surfaces was insignificant in comparison to other effects. This was verified experimentally, as explained in the discussion.

In the cells analyzed here, the important recombination channels then are SRH recombination in the bulk and recombination in the emitter. The total recombination lifetime τ_r resulting from these simultaneously occurring mechanisms can be conveniently expressed as

$$\frac{1}{\tau_r} = \frac{1}{\tau_{SRH}} + \frac{1}{\tau_{emit}} \tag{1}$$

where τ_{SRH} is the SRH bulk recombination lifetime and τ_{emit} an effective emitter recombination lifetime.

The Shockley–Read–Hall bulk lifetime for p-type silicon is calculated via:[15]

$$\frac{1}{\tau_{SRH}} = \frac{N_A + \Delta n}{\tau_{p0}(n_1 + \Delta n) + \tau_{n0}(N_A + p_1 + \Delta n)} \tag{2}$$

Here, Δn is the excess carrier density, N_A the dopant density, n_1 and p_1 the equilibrium densities of electrons and holes, respectively, when the Fermi energy coincides with the recombination centre energy, and τ_{n0} and τ_{p0} the capture time-constants for electrons and holes of the particular SRH centre.

Emitter recombination is determined by:[17]

$$\frac{1}{\tau_{emit}} = \frac{J_{0e}(N_A + \Delta n)}{q n_i^2 W} \tag{3}$$

where J_{0e} is the emitter saturation current density, W the cell thickness and $n_i = 8{\cdot}7 \times 10^9$ cm^{-3} the intrinsic carrier concentration in silicon at 25°C. This is a simplified expression that is only valid when recombination in the emitter is not limited by the transport of carriers from the bulk to the emitter, and a nearly uniform carrier profile exists. It is a good approximation only when J_{0e} is relatively small, or when the contribution of the emitter to the total recombination is small, both of which are true for the cells analyzed here under one-sun operating conditions.

The values of W, N_A and J_{0e} are known by measurement. By adjusting the remaining unknown parameters, namely τ_{n0} and τ_{p0}, a good fit can be obtained for the mid- to high-injection levels. However, a further complicating issue that is important for the mc-Si samples is the presence of trapping centres. These states cause an abnormally large photoconductance at injection levels equal to and less than the

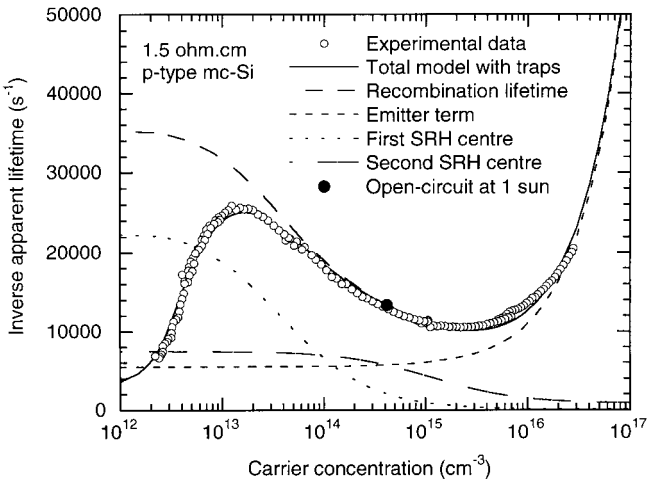

Figure 1. Inverse apparent lifetime vs carrier concentration for a 1·5 Ω cm mc-Si cell precursor. As well as showing the total injection-level dependent model, the constituent parts, namely the two SRH centres and the emitter term, are also shown. The solid circle represents open-circuit conditions under one-sun illumination

trap density (about 1×10^{13} cm^{-3} in these samples), in turn causing the lifetime to increase dramatically with decreasing injection-level.[16,18] Consequently, we refer to the measured lifetime as an 'apparent' lifetime. Such an increase in apparent lifetime does not, however, reflect the true recombination lifetime, and in fact serves only to mask it.[19] This is obviously of significance if we are attempting to use the recombination lifetime to predict final cell parameters such as the open-circuit voltage and fill factor. In order to circumvent this problem, it is possible to fit a trapping model to the apparent lifetime data, with the modeled recombination lifetime as an input, and then 'turn off' the effect of the traps. The details of this procedure are described elsewhere,[16,18] but it essentially involves introducing two more parameters to the fitting process, namely the trap density N_t and the trapping-time to escape-time ratio τ_t/τ_g. This allows the recombination lifetime to be calculated at lower injection-levels than would otherwise be possible. However, the accuracy of such a correction decreases rapidly with decreasing injection-level, and, consequently, the point at which trapping begins to dominate sets an effective lower limit to the injection-levels at which accurate recombination lifetime measurements can be made.

Figure 1 provides an example of a lifetime curve which exhibits all of the features mentioned above. Below 2×10^{13} cm^{-3}, trapping dominates, as indicated by the apparent lifetime increase with decreasing injection-level. Between 2×10^{13} and 2×10^{15} cm^{-3}, the dependence of the lifetime with injection-level is reversed as SRH recombination dominates, while above 2×10^{15} cm^{-3} the dependence is reversed yet again as emitter recombination takes over. Figure 1 also shows the constituent parts as well as the total lifetime model as fitted to the experimental data. The data is plotted in the form of inverse lifetimes in order to make apparent the additive nature of these various components, as expressed by Equation (1). To obtain a good fit, it was necessary to use two independent SRH centres, an emitter term, and the effect of trapping centres. Note that the recombination lifetime is also shown as extrapolated from regions above the onset of trapping to well below it by 'turning off' the traps in the model. As mentioned, the accuracy of such an extrapolation is uncertain, but it serves to show, in qualitative terms, the expected injection-level dependence of the recombination lifetime at lower injection-levels.

With an expression for the injection-level dependence of the recombination lifetime, we can then proceed to predict the open-circuit voltage of a substrate upon metallization. Such predicted open-current voltage vs illumination level data is referred to as an implied illumination-V_{OC} curve. It is possible to predict the open-circuit voltage at all illumination levels, since a knowledge of the lifetime at each illumination level equates to a knowledge of the total carrier densities. We can then write the implied V_{OC} as:[20]

$$V_{OC} = \frac{kT}{q} \ln\left(\frac{\Delta n(N_A + \Delta n)}{n_i^2}\right) \quad (4)$$

It is important to note that an implicit assumption in this method is that the carrier densities do not vary significantly in terms of their spatial profiles in the base, or in other words that the carrier concentration at the junction edge is equivalent to the average carrier density. This generally amounts to requiring the minority carrier diffusion length in the base to be comparable to or larger than the base thickness.

The implied illumination-V_{OC} curve can be compared with the measured illumination-V_{OC} curve after metallization. The short-circuit current density J_{SC} of the cells was measured as a function of illumination, and found to be linear over the measurable range. Consequently, the implied and measured illumination-V_{OC} curves can easily be converted to J_{SC}–V_{OC} curves by using the factors 23·4 and 34·4 mA cm^{-2} sun^{-1} for the 0·4 and 1·5 Ω cm cells, respectively. The large difference between these short-circuit current density values is due to the lack of an antireflection coating on the 0·4 Ω cm cell.

It is possible to take the analysis of the recombination lifetime data further still. Following the method suggested by Sinton,[12] and noting that the currents are linear, the implied illumination-V_{OC} curve, as calculated from the lifetime expression, is converted into an implied one-sun I–V curve by invoking the superposition principle, and neglecting the effects of series resistance. It is then possible to calculate an implied fill factor for each cell. The result will only correlate well with the measured fill factor if the series resistance of the finished cell is negligible at one-sun operation. Such a condition is satisfied for all the cells presented here due to the low resistance ($<0{\cdot}3$ Ω cm^2) of the photolithographically-defined and electroplated front fingers. Note that any reduction in fill factor predicted by the implied I–V curve arises solely from the injection-level dependence of the recombination lifetime, as opposed to shunt or series resistances.

RESULTS AND DISCUSSION

Figures 1 and 2 illustrate lifetime data for two different mc-Si cell precursors, with base resistivities of 1·5 and 0·4 Ω cm. Both show the same general behaviour, being dominated by traps at low injection, then exhibiting some SRH dependence, and finally being dominated by the emitters at high injection.

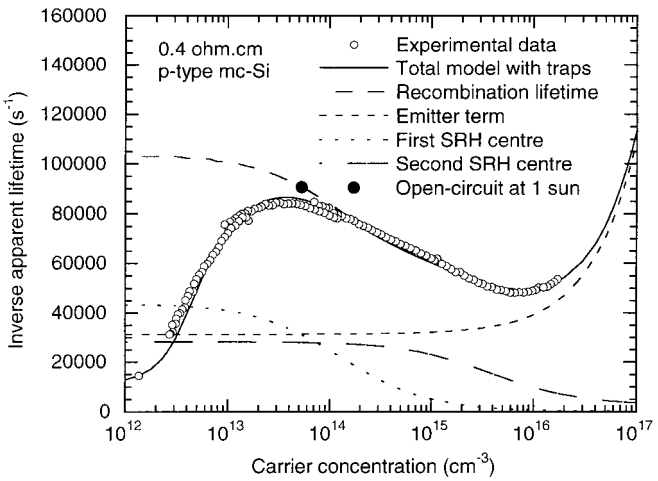

Figure 2. Inverse apparent lifetime vs carrier concentration for a 0·4 Ω cm mc-Si cell precursor. The two SRH curves and the emitter term are shown separately. The solid circle represents open-circuit conditions under one-sun illumination

Table I. Fit parameters for Figures 1 and 2. Two sets of electron- and hole-capture time-constants appear for each sample, since two independent SRH recombination centres were required to obtain a satisfactory fit

Sample type, resistivity	Dopant density N_A (cm^{-3})	Thickness W (cm)	Emitter sat. current J_{0e} (A cm^{-2})	Trap density N_t (cm^{-3})	Trap/escape ratio τ_t/τ_g	Elec.-capt. time-const. τ_{n0} (s)	Hole-capt. time-const. τ_{p0} (s)	τ_{n0}/τ_{p0} ratio
Multi 1·5	$1{\cdot}0\times10^{16}$	0·028	$1{\cdot}9\times10^{-13}$	9×10^{12}	0·02	$3{\cdot}33\times10^{-5}$	$1{\cdot}11\times10^{-2}$	0·003
						$1{\cdot}09\times10^{-4}$	$1{\cdot}09\times10^{-3}$	0·1
Multi 0·4	$4{\cdot}0\times10^{16}$	0·032	$3{\cdot}0\times10^{-13}$	9×10^{12}	0·02	$2{\cdot}13\times10^{-5}$	$7{\cdot}09\times10^{-3}$	0·003
						$3{\cdot}33\times10^{-5}$	$3{\cdot}33\times10^{-4}$	0·1

The lifetime model described above is fitted to both these curves, and also shown separately are the curves due to the SRH centres and the emitter needed to achieve the total fit. Note that it was necessary to employ two SRH centres to achieve a good fit in both cases. In fact it is probable that even more than two types of recombination centres exist in these samples, although two are sufficient to fit within measurement uncertainty. Robinson *et al.*[5] found that the 'kink' in the illumination-V_{OC} curve predicted by their single SRH centre was much sharper than any measured experimentally. They concluded that the presence of more than one type of centre 'smoothed out' the kink. We find a similar situation, but conclude that two centres are sufficient to achieve a kink matched by experiment in this case.

The fit parameters are presented in Table I. It is interesting to notice that the ratio between the electron- and hole-capture time-constants, τ_{n0}/τ_{p0}, for the first and second SRH centres, are the same for the two wafers of different resistivities. These capture time-constants are related to the concentration of SRH recombination centres N_{SRH} and the electron and hole capture cross-sections σ_n and σ_p, which are characteristic of the type of recombination centre, through the relations $\tau_{n0} = 1/(v_{th}\sigma_n N_{SRH})$ and $\tau_{p0} = 1/(v_{th}\sigma_p N_{SRH})$,[15] where $v_{th} = 1{\cdot}1\times10^7$ cm s^{-1} is the thermal velocity of both electrons and holes at 300 K.[21] The fact that these ratios are equal reflects that, although they may be present in varying amounts, the same two types of recombination centre are present for each resistivity. It seems reasonable to expect this to be the case, since the only physical difference between the two samples is the position of the Fermi-level, which does not effect the ratio of the capture time-constants.

The curves of most consequence in Figures 1 and 2 are the recombination lifetime curves, i.e. the sum of the SRH and emitter terms, but with the traps turned off. It is these curves which are later used to calculate the implied illumination-V_{OC} and I–V curves. Note that although trapping drastically affects the photoconductance-based lifetime measurements, it does not have a noticeable effect on cell voltage,[19] which is determined only by the minority carrier recombination lifetime.

At this stage it is important to establish if the SRH dependence arises from surface or bulk states. The front surface can be ruled out, since recombination there is characterized by the emitter term, and has essentially no injection-level dependence in the mid- to low-injection range. Hence, if caused by surface recombination, it must be due to the rear. These substrates enjoy an alnealed oxide on the rear which gives excellent passivation.[8] Single-crystal float zone (FZ) samples processed with the mc-Si samples, of comparable resistivity, yielded effective lifetimes roughly an order of magnitude larger than the mc-Si samples. This suggests that the mc-Si samples are bulk limited, but does not constitute definite proof, since the grain orientations of the mc-Si samples are random and hence the oxide growth is less predictable, potentially leading to poorer passivation.[22] However, when subjected to a corona discharge[23] on the rear oxide, the lifetimes of the FZ wafers increased further due to the field-enhanced passivation, revealing that, although the initial passivation was good, these wafers were rear-surface limited. When a similar charged layer was deposited on the mc-Si wafers, however, no increase was observed. Consequently, we can safely assert that the SRH dependence of the mc-Si samples arises from bulk properties.

Another important feature on these graphs is the solid circle representing the recombination lifetime and injection-level which occur under one-sun illumination. This is the point which determines the

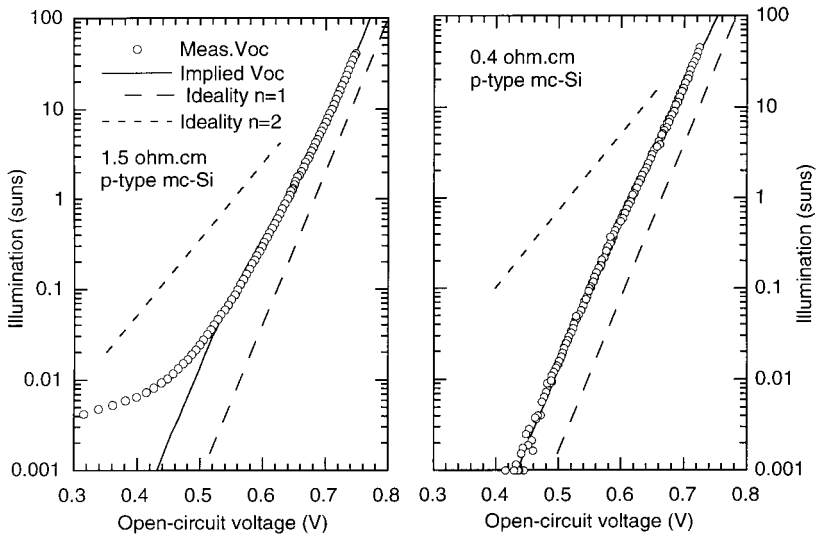

Figure 3. Implied and measured illumination-V_{OC} curves for both the 1·5 Ω cm and 0·4 Ω cm cells. Lines representing idealities of 1 and 2 are included. The effect of a shunt resistance is evident for the 1·5 Ω cm cell at low voltages

Table II. Implied and measured V_{OC} and fill factors (FF) for the two mc-Si cells

Sample	Implied V_{OC} (V)	Meas. V_{OC} (V)	Implied FF	Meas. FF
Multi 1·5	642	644	0·790	0·785
Multi 0·4	616	614	0·827	0·806

open-circuit voltage at one-sun, and the behaviour of the lifetime below this point will influence the fill factor. If the lifetime decreases below the one-sun point, a reduced fill factor will result. For the 1·5 Ω cm substrate, the one-sun point occurs quite near the maximum lifetime, with a strong SRH dependence below. Since there exists a significant injection-level range below the one-sun point that is not affected by trapping, we can use this data to determine the implied illumination-V_{OC} and one-sun I–V curves, and hence predict the fill factor for this cell with some accuracy. Note that this is not so straightforward in the case of the 0·4 Ω cm substrate, for which the onset of trapping occurs very close to one-sun open-circuit conditions, compromising the accuracy of the recombination lifetime measurements around maximum-power conditions.

After lifetime measurements, these substrates were metallized, and the illumination-V_{OC} curves measured. Figure 3 shows the results, together with the implied illumination-V_{OC} data as calculated from the recombination lifetimes. The agreement between the two curves is generally very good, except at illumination levels well below one-sun for the 1·5 Ω cm cell. The one-sun implied and measured V_{OC} for each cell is given in Table II. The large divergence between the data sets at low voltages for the 1·5 Ω cm cell is caused by a shunt resistance that occurred during metallization. The shunt resistance is large enough, however, to not significantly affect the performance of the cell near one-sun maximum-power, and so has little affect on the one-sun fill factor, as verified by numerically fitting a shunt to the illumination-V_{OC} curve.

As a consequence of the shunt, however, the apparent ideality factor for this cell decreases monotonically from values greater than 2 in low voltage regions, towards a value of 1 in high-injection, due

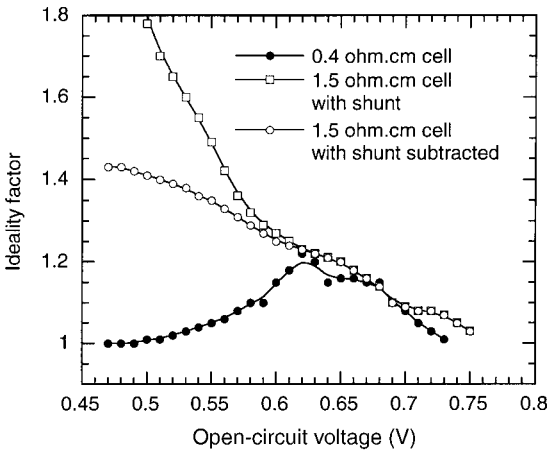

Figure 4. Measured ideality factors for the 1·5 Ω cm (with and without shunt) and 0·4 Ω cm cells. The lines are guides to the eye

to emitter recombination, as shown in Figure 4. Also shown is the ideality for this cell with the effect of the shunt resistance subtracted, revealing that the shunt alone is not sufficient to fully explain the change in ideality. A standard interpretation would be to attribute the non-ideality which is not caused by the shunt to junction recombination, in accordance with the double-diode model.[24,25] However, an alternative explanation would be to attribute such non-ideality to the injection-level dependence of the bulk lifetime, which is precisely what our data suggests. Fortunately, the 0·4 Ω cm cell has no such complicating shunt, and allows us to rule out categorically the influence of junction recombination on the ideality factor. Figure 4 shows that the ideality factor for the 0·4 Ω cm cell is close to unity for low voltages, increases, and then decreases again, in accordance with expectations from the SRH fit to the bulk lifetime data. It is not possible to achieve this type of ideality dependence with a standard double-diode model. We suggest that a similar dependence is occurring in the 1·5 Ω cm cell, but that the low-injection behaviour is masked by the presence of the shunt, leading to a dependence that could be interpreted as junction recombination. Upon subtracting the shunt, the 1·5 Ω cm cell still shows non-idealities at lower voltages than the 0·4 Ω cm cell, but this is due to the more pronounced injection-level dependence below one-sun open-circuit conditions in the 1·5 Ω cm cell.

As further evidence against the presence of junction recombination, we make use of an analytic model that allows an estimation of the magnitude of the recombination current in this part of a device. Corkish and Green[26] developed an expression for an effective upper bound (which they termed $J_{rg}(1)$) on the junction recombination saturation current density J_{rg} (which is the prefactor for the ideality 2 term in the double-diode equation), that holds under the general conditions of asymmetric junctions and capture time-constants. Using the appropriate values as determined for the 1·5 Ω cm cell, we find that $J_{rg} \leqslant 2 \times 10^{-9}$ A cm^{-2}. Under a forward bias of 0·55 V, which is close to maximum-power for the cell in question, this represents a current loss of merely 85 μA cm^{-2}, as compared to the observed loss of more than 1 mA cm^{-2} when compared to a cell with ideality 1 (see Figure 5). Modeling the 0·4 Ω cm cell in a similar way reveals an even smaller effect ($J_{rg} \leqslant 3 \times 10^{-10}$ A cm^{-2}). Remembering that these figures represent upper bounds, it is clear that junction recombination plays a minor role in these devices. This is consistent with other work which concluded that junction recombination is likely to be important only for silicon cells which are thin (< 50 μm) and have very short defect-related lifetimes ($\ll 1$ μs), and which have multiple junctions.[27]

As described above, the implied illumination-V_{OC} data can be used to predict the fill factor of the finished cells via an implied I–V curve. Figure 5 shows the measured and implied I–V curves for the 1·5 Ω cm cell. For the implied curve, the measured value of J_{SC} (34·4 mA cm^{-2}) is used to scale the current axis. Excellent agreement between the measured and implied fill factors can be seen in the values

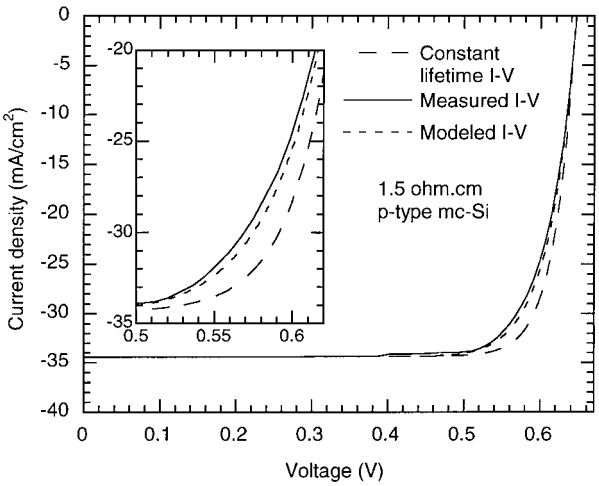

Figure 5. Implied and measured one-sun I–V curves for the 1·5 Ω cm cell. The inset shows a magnified version of the maximum-power region. The constant lifetime I–V curve is for a cell with no injection-level dependence below open-circuit, resulting in a higher fill factor

of 0·785 and 0·790, respectively, as summarized in Table II. Also shown on the figure is the I–V curve expected for a similar cell, but with a constant recombination lifetime below open-circuit conditions. The effects of emitter recombination are retained for high-injection, leading to an ideality of 1 for all injection-levels in this case. This curve represents an 'ideal' cell, and yields a fill factor of 0·835. Thus the low measured fill factor can be attributed to the injection-level dependence of the bulk-lifetime, essentially an intrinsic property of the material, and not to device design problems such as series or shunt resistance, or edge effects, nor to junction recombination. It is interesting to note that the highest efficiency mc-Si cells made to date,[2] on similar 1·5 Ω cm and with a similar cell structure, also achieved a fill factor of 0·795. We suggest that this cell may also have been affected by the injection-level dependence of the bulk lifetime.

The situation is more complicated in the case of the 0·4 Ω cm cell. Table II shows that both the implied and measured fill factor values are larger for the 0·4 Ω cm cell, as compared to the 1·5 Ω cm cell. The basic reason underlying this fact is that the higher dopant density and lower lifetimes cause this cell to be in lower injection, and hence further from the region of strongest SRH dependence. There is, however, a significant disagreement between the implied and measured values for this cell. This is due to our inability to accurately measure the recombination lifetime for this substrate below open-circuit conditions, because of trapping effects. In fact, the lower measured fill factor suggests that the recombination lifetime continues to degrade in the trap-dominated region. It is certainly possible to add further SRH centres to the lifetime model that reduce the lifetime in this region without affecting the fit at higher injection, resulting in a more realistic fill factor. This points to an important general conclusion, in that care must be taken when extrapolating recombination lifetimes into injection levels below the trap density due to the potential changes caused by 'hidden' SRH centres.

It is important to consider here the possible impact of injection-level dependent lifetimes on J_{SC}, as non-linearities in the J_{SC} vs illumination curve would invalidate the use of the superposition principle. For this 1·5 Ω cm cell, the minority carrier diffusion length in the base is always greater than the base thickness, resulting in essentially uniform carrier profiles in the base at all times. It is reasonable then to expect a linear J_{SC} response from this cell, which was verified experimentally by monitoring J_{SC} over a large illumination range. However, the analysis of the 0·4 Ω cm cell is potentially complicated by the fact that the minority carrier diffusion length in the base is less than the base thickness (about half at worst). The result is slightly non-uniform spatial carrier profiles, a situation which is further exacerbated by the injection-level dependent lifetime, and potentially jeopardizes the validity of superposition.

Despite this, the cell exhibited a linear J_{SC} response, indicating that these non-uniformities do not have a significant impact, and are therefore not expected to affect the fill factor. Consequently, we can reasonably state that reduced measured fill factor is a result of the injection-level dependence of the bulk lifetime near maximum-power, even though trapping made accurate modeling impossible.

Injection-level dependent bulk recombination lifetimes are of course not restricted to mc-Si. Boron-doped Czochralski (CZ) silicon, widely used for solar cell applications, is known to suffer from light-induced bulk-lifetime reductions due to boron–oxygen complexes.[28] These complexes exhibit a moderately strong injection-level dependence, and often dominate cell performance. The injection-level dependence of these centres near one-sun maximum-power operation may result in a slightly reduced fill factor in such CZ cells,[29] provided the emitter and surface passivation are sufficient to allow the bulk-lifetime to dominate.

A further example of these effects is provided by FZ wafers which were deliberately cross-contaminated with impurities from mc-Si samples.[30] These contaminated wafers exhibited reduced recombination lifetimes due to the presence of metallic impurities from the mc-Si wafers, and as a consequence of the strong injection-level dependence of the lifetime, resulted in implied V_{OC} curves with idealities of around 1·35 at one-sun.

IMPACT OF INTERSTITIAL IRON ON c-Si CELLS

It is relevant to consider what the physical source of the two SRH centres used to model the lifetimes in the mc-Si cells above might be. The ratios between the electron- and hole-capture time-constants do not coincide well with those expected from the known capture cross-sections for Fe_i, a common metallic lifetime killer in mc-Si,[6] and unfortunately the capture cross-sections are not well known for other metals. Also, considering that the wafers used in these experiments were phosphorus gettered, and the gettering layer was removed before emitter formation, they are consequently expected to have a relatively low interstitial metallic impurity content. We therefore attribute the bulk recombination to metallically decorated crystallographic defects. Such complexes are known to be common in mc-Si and impervious to gettering,[31] but are not currently well characterized in terms of capture cross-sections.

However, standard commercial cell fabrication processes can result in a significant quantity of interstitial metals remaining in the bulk, despite the beneficial gettering effects of emitter and Al back-surface-field formation.[7] By using the capture cross-sections for Fe_i from the literature, we are able to model the effect of different levels of Fe_i contamination on V_{OC} and fill factors. Although the results are specific for Fe_i, many other metallic impurities that reside interstitially in silicon have similar cross-sections. The results then serve the more general purpose of exploring qualitatively the effect of interstitial metallic impurities.

Istratov[32] provides a recent review of Fe complexes in silicon, and suggests the values $\sigma_n = 5{\cdot}0 \times 10^{-14}\text{cm}^2$ and $\sigma_p = 7{\cdot}0 \times 10^{-17}\ \text{cm}^2$ for the electron and hole capture cross-sections for Fe_i at 300 K. The position of Fe_i in the band-gap is taken as 0·4 eV above the valence band, and we also assume a negligible proportion of Fe present in the form of FeB pairs (a safe assumption for cells operating under constant illumination[33]). Figure 6 shows the impact of differing levels of interstitial Fe on V_{OC} and fill factor, for a 1·5 Ω cm cell of thickness 0·03 cm, and with an emitter characterized by a saturation current density of $J_{0e} = 3{\cdot}0 \times 10^{-13}$ A cm^{-2}. Eighty-five per cent of the incoming light is assumed to be coupled into the cell.

There are a number of issues which make the simplified analytic modeling approach used above inappropriate in this case. At higher Fe_i concentrations, the diffusion length of minority carriers in the base becomes significantly less than the cell thickness. This fact, coupled with the strong injection-level dependence of the lifetime due to the highly asymmetrical cross-sections, causes large spatial non-uniformity in the carrier profiles. Also, the expression for emitter recombination becomes less accurate when the cells are dominated by the emitter, due to transport considerations. As a result, we used PC1D[34] to accurately model the impact of Fe_i concentrations on V_{OC} and the fill factor. To ensure only

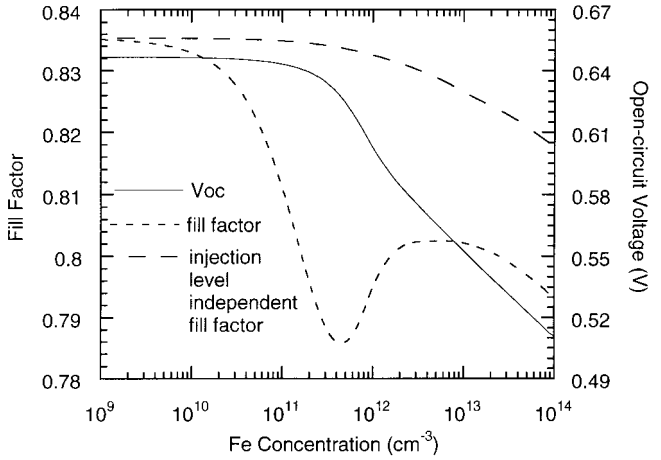

Figure 6. Effect of Fe_i concentration on V_{OC} and fill factor as modeled for a 1·5 Ω cm cell of thickness 0·03 cm and with $J_{0e} = 3 \times 10^{-13}$ A cm^{-2}. Also shown is the fill factor curve for a recombination centre that has an injection-level independent bulk-lifetime

the impact of the bulk-lifetime was being observed, rear surface recombination velocities were set to zero. Junction recombination was verified to have very little impact, with the method described above revealing an upper bound on J_{rg} of about 2×10^{-12} A cm^{-2}, due to the fact that the hole capture cross-section is much larger than that for electrons in the *p*-type side of the junction where the space charge region mostly lies.[26]

The results in Figure 6 show that for Fe_i concentrations below 10^{10} cm^{-3}, the cells are dominated totally by the emitter, which caps the voltage at 647 mV. For such low Fe_i levels, the SRH injection-level dependence is very slight, and the lifetime curve is essentially flat in low injection-levels, resulting in an ideal fill factor of 0·835. As the Fe_i concentration increases though, the fill factor begins to degrade due to the increasing SRH dependence around maximum-power point. As this dependence approaches open circuit conditions, V_{OC} begins to drop also. At around 5×10^{11} cm^{-3}, the strongest part of the SRH dependence is centred near one-sun maximum-power conditions, limiting the fill factor to 0·785. As the Fe_i level increases further still, the lifetime becomes low enough to take the one-sun operating point below the strongest SRH dependence, and the fill factor begins to recover. At these high Fe_i levels, however, the voltage drops off very quickly due to the decreasing bulk-lifetimes.

As the Fe_i concentration increases above 1×10^{12} cm^{-3}, a different effect begins to dominate. The diffusion length in the base is now less than the base thickness, and so the carrier profiles become spatially non-uniform near open-circuit conditions. These non-uniformities give rise, in themselves, to a further reduction of the fill factor. This effect occurs even for the case where the lifetime is injection-level independent. To illustrate this point, Figure 6 also shows the fill factor curve for a recombination centre that has such an injection-level independent lifetime. Clearly it also suffers from fill factor reduction due to spatial non-uniformity. For the case of the Fe_i fill factor curve, the compounding influences of injection-level dependent lifetimes *and* short diffusion lengths result in a large fill factor reduction at high Fe_i concentrations.

The physical reason for the dramatic injection-level dependence of the SRH lifetimes for Fe_i, and hence the poor fill factors, is the large asymmetry between the electron and hole capture cross-sections, which differ by about three orders of magnitude. Other common contaminating metals, notably Cr, have similarly disparate capture cross-sections in the interstitial state. These results then serve to illustrate the detrimental impact metallic impurities can have not only on V_{OC}, but also on the fill factor, and provide a plausible alternative explanation for non-ideal behaviour to junction recombination.

It is interesting to note that a recombination centre which gave rise to the opposite injection-level

lifetime dependence, i.e. a lifetime that *decreases* as the injection-level increases, would result in fill factors *larger* than the constant lifetime case. This would only hold if the lifetime was still large enough to avoid the fill factor reduction associated with spatially non-uniform carrier profiles caused by short diffusion lengths.

CONCLUSIONS

High-efficiency cell designs applied to mc-Si solar cells result in devices whose performance is limited almost wholly by the bulk recombination lifetime, as opposed to single-crystal cells, which tend to be limited by a combination of bulk recombination and surface recombination at the rear oxide. Further improvements in mc-Si cell efficiencies therefore have to stem from increased bulk lifetimes. Treatments such as gettering can help to improve lifetimes, but only to an extent. There still remain bulk recombination centres that cause decreased voltages due to lower lifetimes and also reduced fill factors due to strong injection-level dependence of the lifetime. Consequently, it seems that non-ideal fill factors are often an intrinsic property of the material, and are not always caused by device issues such as series and shunt resistances, nor by junction recombination, which is shown to be of little importance in these cells. The effect of interstitial Fe on the bulk-lifetime injection-level dependence is shown, through modeling, to significantly reduce fill factors, at contamination levels as low as 5×10^{11} cm^{-3}. Any recombination centres that have highly asymmetric capture cross-sections, as many interstitial metals do, will have similar effects.

REFERENCES

1. Stocks M, Blakers A, Cuevas A. Multicrystalline silicon solar cells with low rear surface recombination. *Proceedings of the 26th IEEE PVSC*, Anaheim, CA, 1997; 67.
2. Zhao J, Wang A, Green MA. 19·8% efficient 'honeycomb' textured multicrystalline and 24·4% monocrystalline silicon solar cels. *Appl. Phys. Lett*. 1999; **73**: 1991.
3. Aberle AG, Altermatt P, Heiser G, Robinson S, Wang A, Zhao J, Krumbein U, Green MA. Limiting loss mechanisms in 23% efficient silicon solar cells. *J. Appl. Phys*. 1995; **77**: 3491.
4. Aberle AG, Robinson S, Wang A, Zhao J, Wenham SR, Green MA. High efficiency silicon solar cells: fill factor limitations and non-ideal diode behaviour due to voltage-dependent rear surface recombination velocity. *Progress in Photovoltaics* 1993; **1**: 133.
5. Robinson S, Aberle AG, Green MA. Recombination saturation effects in silicon solar cells. *IEEE Trans. Elec. Devices* 1994; **41**: 1556.
6. Hopkins RH, Rohatgi A. Impurity effects in silicon for high efficiency solar cells. *J. Cryst. Growth* 1986; **75**: 67.
7. Elgamel H. High efficiency polycrystalline silicon solar cells using low temperature PECVD process. *IEEE Trans. Elec. Devices* 1998; **45**: 2131.
8. Cuevas A, Stocks M, Macdonald D, Kerr M, Samundsett C. Recombination and trapping in multicrystalline silicon. *IEEE Trans. Elec. Devices* 1999; **46**: 2026.
9. Sinton RA, Cuevas A. Contactless determination of current-voltage characteristics and minority-carrier lifetimes in semiconductors from quasi-steady-state photoconductance data. *Appl. Phys. Lett*. 1996; **69**: 2510.
10. Nagel H, Berge C, Aberle AG. Generalized analysis of quasi-steady-state and quasi-transient measurements of carrier lifetimes in semiconductors. *J. Appl. Phys*. 1999; **86**: 6218.
11. Mimura M, Ishikawa S, Saitoh T. Effect of thermal annealing on minority-carrier lifetimes for multicrystalline silicon wafers. *Technical Digest of 11th International Photovoltaic Science and Engineering Conference*, Hokkaido, Japan, 1999; 357.
12. Sinton RA. Possibilities for process-control monitoring of electronic material properties during solar cell manufacture. *Ninth Workshop on Crystalline Silicon Solar Cell Materials and Processes*, Colorado, 1999; 67.
13. Shockley W, Read WT. Statistics of the recombinations of holes and electrons. *Phys. Rev*. 1952; **87**: 835.
14. Hall RN. Electron-hole recombination in germanium. *Phys. Rev*. 1952; **87**: 387.

15. Smith RA. *Semiconductors*. Cambridge University Press: Cambridge, 1959.
16. Macdonald D, Cuevas A. Boron-related minority-carrier trapping centers in p-type silicon. *Appl. Phys. Lett*. 1999; **75**: 1571.
17. Cuevas A. The effect of emitter recombination on the effective lifetime of silicon wafers. *Solar Energy Mat. and Solar Cells* 1999; **57**: 277.
18. Macdonald D, Cuevas A. Trapping of minority carriers in multicrystalline silicon. *Appl. Phys. Lett*. 1999; **74**: 1710.
19. Macdonald D, Cuevas A. A study of carrier trapping in multicrystalline silicon. *Technical Digest of 11th International Photovoltaic Science and Engineering Conference*, Hokkaido, Japan, 1999; 361.
20. Cuevas A, Sinton RA. Prediction of the open-circuit voltage of solar cells from the steady-state photoconductance. *Progress in Photovoltaics* 1997; **5**: 79.
21. Bullis WM, Huff HR. Interpretation of carrier recombination lifetime and diffusion length measurements in silicon. *J. Electrochem. Soc*. 1996; **143**: 1399.
22. Stocks M, Cuevas A. Surface recombination velocity of thermally oxidized multicrystalline silicon. *Proceedings of the 2nd World Conference on Photovoltaic Energy Conversion*, Vienna, Austria, 1998; 1623.
23. Schofthaler M, Brendel R, Langguth G, Werner JH. High-quality surface passivation by corona-charged oxides for semiconductor surface characterisation. *Proceedings of the 1st World Conference on Photovoltaic Energy Conversion*, Hawaii, 1994; 1509.
24. Wolf M, Noel G, Stirn R. Investigation of the double exponential in the current-voltage characteristics of silicon solar cells. *IEEE Trans. Elec. Devices* 1977; **24**: 419.
25. Charles J-P, Bordure G, Khoury A, Mialhe P. Consistency of the double exponential model with the physical mechanisms of conduction for a solar cell under illumination. *J. Phys. D: Appl. Phys*. 1985; **18**: 2261.
26. Corkish R, Green MA. Junction recombination current in abrupt junction diodes under forward bias. *J. Appl. Phys*. 1996; **80**: 3083.
27. Stocks MJ, Cuevas A, Blakers AW. Theoretical comparison of conventional and multilayer thin silicon solar cells. *Progress in Photovoltaics* 1996; **4**: 35.
28. Schmidt J, Cuevas A. Electronic properties of light-induced recombination centers in boron-doped Czochralski silicon. *Journal of Applied Physics* 1999; **86**: 3175.
29. Schmidt J. Personal communication.
30. Cuevas A, Macdonald D. Lifetime studies of multicrystalline silicon. *Eighth Workshop on Crystalline Silicon Solar Cell Materials and Processes*, Copper Mountain, Colorado, 1998; 57.
31. McHugo S, Thompson A, Perichaud I, Martinuzzi S. Direct correlation of transition metal impurities and minority carrier recombination in multicrystalline silicon. *Appl. Phys. Lett*. 1998; **72**: 3482.
32. Istratov AA, Hieslmair H, Weber ER. Iron and its complexes in silicon. *Appl. Phys. A* 1999; **69**: 13.
33. Zoth G, Bergholz W. A fast, preparation-free method to detect iron in silicon. *J. Appl. Phys*. 1990; **67**: 6764.
34. Basore PA, Clugston DA. PC1D V5·3. 1998.

